Journal of the Nigerian Association of Mathematical Physics,
Volume 8, (***November 2004***)

Pressure transient analysis of a horizontal well subject to four vertical well injectors

E. S. Adewole and **K .O. Bello**
Department of Petroleum Engineering,
University of Benin, Benin City, Nigeria

Abstract

Reservoir characterization is essential for effective reservoir and wellbore management. But when a horizontal well is subject to constant-pressure external boundaries, the extent of reservoir characterization that is possible depends on the flow regimes that are encountered in a given flow time. In this paper dimensionless pressure distribution of a horizontal well oil producer, subject to four vertical well fluid injectors, is utilized to identify the possible flow regimes in the horizontal well. The study shows that the number of flow regimes identifiable depends on the permeability distribution and geometry of the reservoir. In particular, for a square shaped reservoir with central horizontal well location, only two major flow regimes are identifiable. More flow regimes may occur if the reservoir length is at least one log cycle greater than the breadth, and the horizontal permeability is substantially high.

pp 75 - 82

1.0 Introduction

When a horizontal well is producing under fluid injection drive by four vertical wells in a rectangular pattern, the horizontal wellbore pressure may exhibit several flow regimes. By implication, therefore, test analysis using flow pressures from the horizontal well will depend on the flow regimes attained during the test time. One flow regime that is certain is the early radial flow regime. This is unaffected by reservoir boundary conditions. More often than not, flow transients are sooner curbed by the emergence of injected fluid in the production (horizontal) well. This precipitates a steady-state flow situation, which eventually leads to injected fluid breakthrough. Depending on the reservoir permeability distribution, wellbore and reservoir geometry and flow rates, the injectors may communicate with the horizontal well at different times. This means that the emergence of a steady-state flow may not fully characterize the reservoir, and so is the analysis performed for the same test period. It is therefore very necessary to isolate all the possible flow regimes for correct analysis of pressure data.

To achieve this aim, a dimensionless pressure distribution model is derived for a reservoir with constant-pressure external boundaries. Possible flow regimes encountered, owing to unsteady production of oil, and modalities for identifying each regime will be discussed. Useful information obtainable from each regime will be sought.

In the literature, several authors [1-4] have discussed horizontal well test analysis for reservoirs with varied boundaries. What is most commonly discussed for horizontal wells with constant-pressure boundaries are the critical oil production rate [5-6], fluid breakthrough time [7-10] and displacement efficiency [10]. That is, the major concern has been the effect of the movement of oil-water or gas-oil interface, whether these boundaries are natural or artificial (fluid injection). The particular case of interest in this paper is similar to a normal 5-spot injection/production pattern, but where the producer is a horizontal well. The patterns where all the wells are vertical are discussed extensively in [Ref. 11]. The dimensionless pressure distributions are derived using Green's and source functions derived in Refs. [12 and 13].

2.0 Reservoir and Mathematical Models Descriptions

A horizontal well is located in the center of an anisotropic reservoir which has four vertical injectors drilled in a pattern similar to a quadrilateral geometry as shown in Figure 1. The reservoir

pressure is p_e initially, and the horizontal well is allowed to produce at a constant rate, q, while maintaining equal and constant injection rates, $-q$, at the four vertical wells. Subsequently, in accordance with production and injection, the reservoir pressure changes with time until production is completely balanced by injection. It is assumed that the reservoir contains oil of small but constant compressibility. The only sources of energy for oil flow therefore

are dissolved gas and fluid injection. A relationship between the wellbore and reservoir parameters with time will be derived to understand fluid flow in such a reservoir system. Furthermore, it is assumed that the horizontal well is located in the middle of the lateral extent of the reservoir and has Length, L (along the x-axis), and width y_w (along the y-axis).

The reservoir has permeability values k_x, k_y *and* k_z in the x, y, and z- directions, respectively, and has a bulk volume $x_e y_e h$ because it is h ft thick (in the z-direction). The horizontal well is centered at point $(x,y,z) = (x_w, y_w, z_w)$. Skin and wellbore storage effects are not considered. Reservoir description is achieved under flow condition of unit mobility ratio. This condition guarantees that there is no injected fluid breakthrough into the producing well.

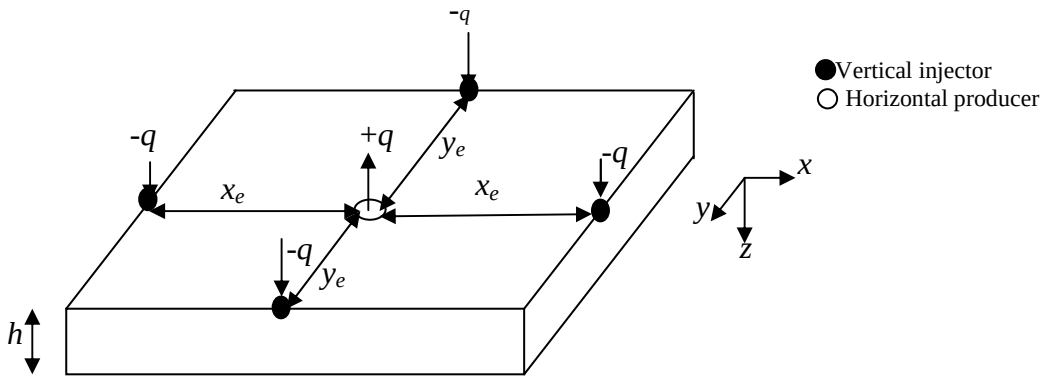

Figure1: Reservoir Model consisting of Four Vertical Injectors and One Horizontal Producer

Following the description above and the external sources of flow energy, the horizontal well experiences an infinite slab source from an infinite slab reservoir with prescribed pressure on both sides (along the x-axis); an infinite plane source from an infinite slab reservoir with prescribed pressure boundaries (along the y-axis), and an infinite plane source in an infinite slab reservoir with a constant pressure boundary at the top. These source functions are written as follows:

(1) ***x*-axis**

$$s(x_D, t_D) = \frac{4}{\pi}\sum_{n=1}^{\infty}\frac{1}{n} exp\left(-\frac{n^2\pi^2 t_D}{x_{eD}^2}\right) \sin n\frac{\pi}{x_{eD}} \sin n\pi\frac{x_{wD}}{x_{eD}} \sin n\pi\frac{x_D}{x_{eD}} \qquad (2.1)$$

(2) ***y*-axis**

$$s(y_D, t_D) = \frac{2}{y_{eD}}\sum_{l=1}^{\infty} exp\left(-\frac{l^2\pi^2 t_D}{y_{eD}^2}\right) \sin l\pi\frac{y_{wD}}{y_{eD}} \sin l\pi\frac{y_D}{y_{eD}} \qquad (2.2)$$

(3) ***z*-axis**

$$s(z_D, t_D) = \frac{2}{h_D}\sum_{m=1}^{\infty} exp\left(-\frac{(2n+1)^2\pi^2 t_D}{4h_D^2}\right) cos(2n+1)\pi\frac{z_{wD}}{h_D} cos(2n+1)\pi\frac{z_D}{h_D} \qquad (2.3)$$

With these source functions the dimensionless pressure is written as follows using the Newman's method [12]

$$p_D(x_D, y_D, z_D, \tau_D) = 2\pi h_D \int_0^{t_D} s(x_D, \tau_D).s(y_D, \tau_D)s(z_D, \tau_D)\, d\tau_D \quad (2.4)$$

for a constant oil production rate. Substituting equations (2.1) to (2.3) into equation (2.4) we have:

$$p_D(x_D, y_D, z_D, \tau_D) = \frac{32}{y_{eD}} \int_0^{t_D} \left[\sum_{n=1}^{\infty} \frac{1}{n} exp(-\frac{n^2\pi^2\tau_D}{x_{eD}^2}) sinn\frac{\pi}{x_{eD}} sinn\frac{x_{wD}}{x_{eD}} sinn\frac{x_D}{x_{eD}} \right] .$$
$$\left[\sum_{l=1}^{\infty} exp(-\frac{l^2\pi^2\tau_D}{y_{eD}^2}) sinl\pi\frac{y_{wD}}{y_{eD}} sinl\pi\frac{y_D}{y_{eD}} \right] .. \quad (2.5)$$
$$\sum_{m=1}^{\infty} exp(-\frac{(2m+1)^2\pi^2\tau}{4h_D^2}) cos(2m+1)\pi\frac{z_{wD}}{h_D} cos(2m+1)\pi\frac{z_D}{h_D} d\tau_D$$

The dimensionless parameters are defined based on wellbore half-length as:

$$i_D = \frac{2i}{L}\sqrt{\frac{k}{k_x}} \quad (2.6)$$

where $i = x, y,$ or z-axis

$$L_D = \frac{L}{2h}\sqrt{\frac{k}{k_x}} \quad (2.7)$$

$$h_D = \frac{2h}{L}\sqrt{\frac{k}{k_z}} \quad (2.8)$$

$$t_D = \frac{4kt}{\phi\mu c L^2} \quad (2.9)$$

$$p_D = \frac{2\pi k h \Delta p}{q\mu}. \quad (2.10)$$

$$\tau_D = \frac{4k\tau}{\phi\mu c L^2} \quad (2.11)$$

For flow observation using the horizontal well, equation (2.5) shows that the most likely flow regimes are: (1) an early radial (2) an early steady state and (3) a late steady state

2.1 Early radial flow regime

During this period the effects of the four vertical injectors and all the lateral and vertical boundaries have not been felt. That is, the horizontal well flow is still like a fully penetrating vertical well in a reservoir of thickness L. Therefore, the dimensionless pressure distribution during this flow period is written as follows:

$$p_D(x_D, y_D, z_D, \tau_D) = \frac{h_D}{8}\sqrt{\frac{k^2}{k_y k_z}} \int_0^{t_D} \left[erf\left(\frac{\sqrt{k/k_x} + x_D}{2\sqrt{\tau_D}}\right) + erf\left(\frac{\sqrt{k/k_x} - x_D}{2\sqrt{\tau_D}}\right) \right] . \quad (2.12)$$
$$\frac{e^{-\left[(y_D - y_{wD})^2 + (z_D - z_{wD})^2\right]/4\tau_D}}{\tau_D} d\tau_D$$

Equation (2.12) is predicated on the fact that the source functions given in equations (2.1) to (2.3) are represented by their early time equivalents [12, 13] given the reservoir description and well location. The general solution to equation (2.12) is :

$$p_D(x_D, y_D, z_D, t_D) = -\frac{\alpha h_D}{8}\sqrt{\frac{k^2}{k_y k_z}} Ei\left[-\frac{(y_D - y_{wD})^2 + (z_D - z_{wD})^2}{4t_D}\right] \quad (2.13)$$

where $\alpha = 2$ if $\sqrt{(k/k_x)} > x_D$, 1 if $\sqrt{(k/k_x)} = x_D$, and 0 if $\sqrt{(k/k_x)} < x_D$.

This period must prevail irrespective of the nature of the external boundaries of the reservoir.

2.2 Early steady state flow regime

This period may not occur if the well length is long in relation to the reservoir thickness. It may occur, however, if the wellbore length is short compared with the reservoir thickness (this is a rare possibility), and the horizontal permeability is larger than vertical permeability. If it does occur, then according to equation (2.4), the dimensionless pressure distribution is written as:

$$p_D(x_D, y_D, z_D, \tau_D) = h_D \int_0^{t_D} \sum_{n=1}^{\infty} \frac{1}{n} exp(-\frac{n^2\pi^2\tau_D}{x_{eD}^2}) \sin n\pi \frac{1}{x_{eD}} \sin n\pi \frac{x_{wD}}{x_{eD}} \sin n\pi \frac{x_D}{x_{eD}} \cdot \frac{e^{-[(y_D - y_{wD})^2 + (z_D - z_{wD})^2]/4\tau_D}}{\tau_D} d\tau_D \quad (2.14)$$

But in the former case, where the well length is long in relation to the reservoir thickness, if there is a better vertical permeability than the horizontal permeability, the effects of injection along the *y*- and *z*-axes are felt while the transients from the *x*-axis remain infinite-acting. Thus, the dimensionless pressure distribution for this regime is written as:

$$p_D(x_D, y_D, z_D, \tau_D) = \frac{\pi}{2y_{eD}} \int_0^{t_D} \left[erf(\frac{\sqrt{k/k_x} + x_D}{2\sqrt{\tau_D}}) + erf(\frac{\sqrt{k/k_x} - x_D}{2\sqrt{\tau_D}}) \right] \cdot \sum_{l=1}^{\infty} exp(-\frac{l^2\pi^2\tau_D}{y_{eD}^2}) \sin l\pi \frac{y_{wD}}{y_{eD}} \sin l\pi \frac{y_D}{y_{eD}} \cdot \sum_{m=1}^{\infty} exp(-\frac{(2m+1)^2\pi^2\tau_D}{4h_D^2}) \cos(2m+1)\pi \frac{z_{wD}}{h_D} \cos(2m+1)\pi \frac{z_D}{h_D} . d\tau_D \quad (2.15)$$

The period of occurrence of this regime and the late steady-state period may be indistinguishable in terms of real pressure behavior. Once any of these steady-states manifests, it prevails throughout the entire flow period because changes in pressure gradients cease to occur.

2.3 Late steady-state flow period

Finally, the pressure transient felt in the horizontal wellbore is now contributed from all the injectors. This will be evident by a final and permanent steady-state manifestation. The dimensionless pressure distribution during this period corresponds to equation (2.5). Although, it exhibits the same flow characteristics like an early steady state, it may be recognized by a unique dimensionless pressure distribution for a rectangular flood pattern, where either $x_{eD} >> y_{eD}$ or $x_{eD} << y_{eD}$. This will, however, be shown later.

2.4 Periods of attainment of steady-state

At early radial flow period, the dimensionless pressure distribution in the horizontal well would exhibit dimensionless pressure gradients (with dimensionless flow time) typical of infinite flow. At full steady state, the dimensionless horizontal well pressure becomes uniform because of the recharge from external boundaries. At this time, injected fluid is now replacing the produced fluid in the pores of the reservoir. The cumulative production rate can then be used to calculate the amount of oil produced from onset of production to-date (at which dimensionless time the last steady-state period is attained). From equation (2.12) only infinite flow characteristics will be exhibited. From equation (2.13), the first steady-state behavior will set in at t_D corresponding to $\partial p_D/\partial t_D = 0$. That is, at

$$t_{Dss} \geq \frac{x_{eD}^2}{\pi^2} \quad (2.16)$$

Similarly, by solving equation (2.15) for $t_D = t_{Dss}$, a second steady-state period may manifest at

$$t_{Dss} \geq max.\left\{\frac{y_{eD}^2}{\pi^2}, \frac{4h_D^2}{3\pi^2}\right\}. \quad (2.17)$$

and, finally from equation (2.5), the final steady-state period is attained at

$$t_{Dss} \geq max.\left\{\frac{x_{eD}^2}{\pi^2}, \frac{y_{eD}^2}{\pi^2}, \frac{4h_D^2}{3\pi^2}\right\} \quad (2.18)$$

It should be noted that these dimensionless times of attainment of steady state are (1) approximate, (2) from start of production to date, and (3) generally earlier than the corresponding dimensionless breakthrough times. Infinite-acting dimensionless times for any geometry are less than their equivalent t_{Dss}. In all the flow periods or regimes, solution to equation (2.13) prevails throughout the flow period. Therefore, for any of the other regimes, the final dimensionless pressure distribution is a superposition of this solution and the solution at early radial period. In practice, if flow rate is large and k_z is also large, the dimensionless times of attainment of steady-state may be indistinguishable from one another.

3.0 Well test analysis

Once a pressure profile is obtained for any period, type-curve matching is recommended for analysis. The type curves are prepared using equations (2.5), (2.14), or (2.15).

3.1 Information derivable *from the flow regimes*

3.1.1 Early radial flow regime

Flow is basically in the y-z plane. Therefore, k_y , k_z, near wellbore effects, such as skin due to damage or repair and partial penetration can be estimated, if more than one well test data are analyzed. More than one well test data analyses are required because these effects were not part of the flow model originally. A master type-curve of p_{wD} against t_D is matched and analyzed to obtain reservoir and fluid properties during this period

[14]. A draw down test analysis using the master curves can give the volume of reservoir oil in communication with the wellbore [15]. The wellbore productivity index, *PI*, can also be calculated using Δp_{ss} and the corresponding production rate [6].

3.1.2 Early steady-state flow regime

This regime still yields k_y and k_z or k, using the trend on the type-curve just before the emergence of steady state. However, the correct wellbore productivity index, *PI*, cannot be estimated now. This period is actually transitional, and therefore, does not show the real character of the reservoir. But, whichever of these two variations of flow (early or late steady-state) that is achieved first shows the nearness of the influencing boundary or the larger of k_y and k_z.

3.1.3 Late steady-state flow regime

Using the early part of this flow regime, the information described above can also be obtained. Additionally, because all the reservoir boundaries are now felt, the reservoir pressure p_e, can be estimated from the stabilized observed wellbore pressure. Therefore, the reservoir pressure decline, p_I-p_{ss} , psi since production commenced can be calculated if there is no effective communication yet between the injector and producer; for instance, if the reservoir exhibit dual porosity and is extensively heterogeneous. Finally, k_x, k_y, k_z or k can be obtained from the trend just before this period starts.

4.0 Computation of dimensionless pressures

Most authors usually write approximate expressions to predict the end of infinite flow. In most cases of horizontal well applications, the vertical boundary is the first to create influence that curbs infinite behaviour because it is the nearest. In the case studied here, the vertical boundary is a constant-pressure boundary and would therefore produce a constant pressure effect with time. This will occur at $t_D = t_{Dss} = 4h_D^2/3\pi^2$. The period between end of infinite flow and t_{Dss} may be short but is very useful in estimating the reservoir properties. In computing wellbore dimensionless pressures, p_{wD}, $y_D = y_{wD}$ (line source well), $z_D = z_{wD} + r_{wD}$ *and* $r_{wD} = y_{wD}$. Any other p_D is computed based on the position of interest along the well length or elsewhere in the reservoir. Infinite conductivity is simulated by assuming x_D = 0.732 91, [1,4]. The well

is centered at x_{wD}, $y_D = y_{wD}$ and $z_D = z_{wD}$, *where* $x_{wD} \leq x_D$ *or* $x_{wD} \geq x_D$ along the well length. All integrals were evaluated numerically [16].

5.0 Results and Discussion

Results of p_{wD} at varying t_D and for different wellbore parameters for the early radial flow period are shown in Table 1.

Table 1: Dimensionless Wellbore Pressure, p_{wD}, at Early Radial Period z_{wD}=0.5, L_D =1.0 (h_D = 1.0), infinite conductivity case

t_D	$r_{wD} = 5\times 10^{-5}$	$r_{wD} = 10^{-4}$	$r_{wD} = 5\times 10^{-4}$	
			Equation. (2.13)	Ref. [4]
10^{-4}	2.851	2.5049	1.7001	1.700
10^{-3}	3.427	3.0805	2.2758	2.276
10^{-2}	4.000	3.6562	2.8514	2.849
10^{-1}	4.501	4.2318	3.4271	3.350
1	5.212	4.9587	4.1940	4.060

5.1 Early steady-state dimensionless pressures

Considering a rectangular reservoir geometry where x_{eD} = 10 and y_{eD} = 20, then from equation (2.18) the last steady-state period would start at $t_{Dss} \geq 40.53$. The earliest steady-state may start at $t_{Dss} = 4h^2_D/3\pi^2$ (or 1.35 x10^{-1}) or, at $t_{Dss} = x^2_{eD}/\pi^2$ (or 10.132), immediately after the infinite-acting period. If steady-state occurs first at t_{Dss} =1.35x10^{-1}, then Table 2 shows the dimensionless wellbore pressure distribution to be observed.

Table 2: Dimensionless Pressure p_D if the h_D =1.0 upper const ant pressure boundary is felt first

t_D	r_{wD} =5x10^{-5}	10^{-4}	5x10^{-4}
10^{-4}	2.851	2.5049	1.7001
10^{-3}	3.427	3.0805	2.2758
10^{-2}	4.000	3.6562	2.8514
10^{-1}	4.451	4.2070	3.4021
1	4.451	4.2070	3.4021

But if the x_{eD}=10 constant pressure boundary is felt first the dimensionless wellbore, wellbore pressure distribution is shown in Table 3. The results of p_D at t_D for the example data are the same as shown in Table 3 even if the constant-pressure boundary at y_{eD} =20 is felt first. This is as a result of the occurrence of steady-state within the same log cycle as x_{eD} =10. Assuming the reservoir is a square, the same results will also be obtained for the same reason. But, if x_{eD} = 10 and $y_{eD} \geq 32$ there is a possibility of a distinct pressure distribution given by equation (2.15), from that given by equation (2.14), because equation (2.14) yields an earlier steady-state at t_D =10 while infinite behavior continues beyond t_D =10 for x_{eD} =10 and $y_{eD} \geq 32$ according to Eq.(2.15). The p_D for the second early steady-state is shown in Table 4.

5.2 Late steady-state dimensionless pressure distribution

For x_{eD}=10 and $y_{eD} \geq 100$, another unique pressure distribution, shown in Table 5 is obtained using equation (2.5). That is, the late steady state pressure distribution will be observed when $\frac{y^2_{eD}}{\pi^2} \geq max.\left\{\left|\frac{x^2_{eD}}{\pi^2}, \frac{3h^2_D}{4\pi^2}\right.\right\}$ by at least one log cycle, (between t_D=10^2 and 10^3).

Table 3: Dimensionless Pressure p_D if the x_{eD}=10 constant pressure boundary is felt first

t_D	$r_{wD} = 5\times10^{-5}$	$r_{wD} = 10^{-4}$	$r_{wD} = 5\times10^{-4}$
10^{-4}	2.851	2.5049	1.7001
10^{-3}	3.427	3.0805	2.2758
10_{-2}	4.000	3.6562	2.8514
10^{-1}	4.501	4.2318	3.4271
1	5.212	4.9987	4.1940
10	6.4712	6.005	5.3199
100	6.4712	6.005	5.3199

Table 4: Dimensionless Pressure p_D if the $x_{eD} = 10$, $y_{eD} \geq 32$ const ant-pressure boundaries are felt first

t_D	$r_{wD} = 5\times10^{-5}$	10^{-4}	5×10^{-4}
10^{-4}	2.851	2.5049	1.7001
10^{-3}	3.427	3.0805	2.2758
10^{-2}	4.000	3.6562	2.8514
10^{-1}	4.501	4.2318	3.4271
1	5.212	4.9987	4.1940
10	6.4712	6.005	5.3199
100	7.4180	7.0710	6.2660
1000	7.4180	7.0710	6.2660

Table 5: Late Steady-State Flow Dimensionless Pressure Distribution, $p_D x_{eD} = 10$, $y_{eD} = 100$

t_D	$r_{wD} = 5\times10^{-5}$	10^{-4}	5×10^{-4}
10^{-4}	2.851	2.5049	1.7001
10^{-3}	3.427	3.0805	2.2758
10^{-2}	4.000	3.6562	2.8514
10^{-1}	4.501	4.2318	3.4271
1	5.212	4.9987	4.1940
10	6.4712	6.0050	5.3199
10^2	7.4180	7.0710	6.2660
10^3	8.5680	8.221	7.417
10^4	8.5680	8.221	7.417

The dimensionless time at which fluid breakthrough is observed and the particular pressure distribution obtained serve very useful project assessment hints. As stated earlier, the appearance of one steady-state contributed from any part of the reservoir, means that the other injectors would not be opportune to exert their influence. This is because at steady-state, which eventually leads to breakthrough, no meaningful pressure drop occurs in the reservoir any more. Hence, it becomes difficult to notice contributions from the remaining injectors. The obvious advantage of this behavior is that the contributing injectors can be identified given the prevailing dimensionless pressure profile and dimensionless time of attainment of steady-state. Therefore, it is pertinent to judge that (1) If the observed dimensionless pressure corresponds to those in Table 1, then the horizontal wellbore flow is still in the infinite acting regime; that the influence of any of the injectors has not been felt by the horizontal well. Clean oil is therefore expected to be produced throughout this time of prevalence of this regime. (2) If the observed dimensionless pressure and time of attainment of steady-state match those in Table 2, then only the top of the reservoir is contacted and therefore swept by injection. This means that there is no effective sweep of the reservoir along the x- and -y-axes. Oil production will therefore be limited to that swept from the top of the reservoir. The only occasion when this occurrence may be advantageous is when the horizontal producer is located very close to or at the base of the pay zone, i.e., at $z_{wD} = 0$. Then will there be a large volume of oil to be moved before steady-state is attained (3) Attainment of the results in Table 3 means that, if $x_{eD} > h_D$, either $k_h > k_V$ or the top of the reservoir is not effectively swept by injection. Otherwise, the trend shows

that the lateral extent of the reservoir is swept effectively and the injectors along the y-axis (where $y_{eD} >> x_{eD}$) did not contribute significantly to oil displacement. (4) The dimensionless pressure distributions in Table 4 or 5 show that the injectors at the farthest extent of the reservoir (i.e., at $y_{eD} \geq 32$ or 100) contributed to oil displacement without injection fluid breakthrough. This implies therefore that optimum oil recovery is achieved.

6.0 Conclusion

All the possible flow regimes of a horizontal well subject to four vertical injectors have been identified. Numerical computations showed that the number of flow regimes observable depends on the reservoir geometry. These are (1) an infinite flow regime (2) transition flow regime and (3) final steady-state flow regime. Each of the flow regimes offers unique characteristics that can be used to estimate both wellbore and reservoir properties. For a square reservoir geometry, only the infinite and the final (late) steady-state periods are observable. When the reservoir length is much larger than the width, then there is a possibility of more than two flow regimes.

Nomenclature

c	*compressibility, 1/psi*
k	*permeability, md*
h	*pay thickness, ft*
i	*distances either in x,y, or z directions, ft*
p	*pressure, psi*
psi	*pounds per square inch*
q	*production / injection rate, STB/ D*
r	*radius, ft*
t	*time, hours*
s	*source*
STB/D	*stock tank barrel per day*
L	*well length, ft*
ϕ	*porosity, fraction*
μ	*viscosity , cp*
τ	*dummy integration variable for time*

Subscripts

D	*dimensionless*
h	*orizontal*
t	*total*
e	*xterna*
v	*vertical*
w	*wellbore*

References

[1] Goode, P.A and Thambynayagam, R.K.M.: "Pressure Drawdown and Buildup Analysis for Horizontal Wells in Anisotropic Media," *SPE Formation Evaluation*, p. 683-697, Dec. 1987.

[2] Davian, F., Mouronval, G., Bourdarot, G. and Curutchet, P.: "Pressure Analysis for Horizontal Wells," *SPE Formation Evaluation*, p. 716-724, Dec. 1988.

[3] Odeh, A.S. and Babu, D.K.: "Transient Flow Behaviour of Horizontal Wells: Pressure Drawdown and Buildup Analysis," *SPE Formation Evaluation*, P. 7-15, March 1990.

[4] Ozkan, E., Raghavan, R. and Joshi, S.D.: "Horizontal-Well Pressure Analysis," *SPE Formation Evaluation*, p. 567-575, Dec. 1989.

[5] Kuchuk, F.J. et al.: " Pressure Transient Behaviour for a Horizontal Well with and without Gas cap or Aquifer," paper SPE 17413 presented at the 1988 SPE California Regional Meeting, Long Beach, March 23-25.

[6] Papatzacos, P.: "Gas Coning by a Horizontal Well," Well-Test Analysis, Rogaland Research Inst., Stravanger (March 1989) Report K. 63/89.

[7] Papatzacos, P., Herring, T.R., Martinsen, R. and Skjaeveland, S.M.: "Cone Breakthrough Time for Horizontal Wells," *SPERE, Trans*, AIME (Aug. 1991) 291, 311- 318.

[8] Papatzacos, P.: "Gas Coning by a Horizontal Well as a Moving Boundary Problem," *Proc*., European Conference on Mathematics of Oil Recovery Cambridge (July 25-27, 1989).

[9] Giger, F.M.: " Analytic 2-D Models of Water Cresting before Breakthrough for Horizontal Wells," *SPERE*, p. 409-416, Nov. 1989.

[10] Ozkan, E. and Raghavan, R.: " Performance of Horizontal Wells Subject to Bottom Water Drive," paper SPE 18545, presented at the SPE Eastern Regional Meeting, Charleston, West Virginia, Nov. 2-4, 1988.

[11] Craig, F.F.: *Reservoir Engineering Aspects of Waterflooding* Society of Petroleum Engineers Monogragh, 1962.

[12] Gringarten, A.C and Ramey, H.J. Jr.: " The Use of Source and Green's Functions in Solving Unsteady Flow Problems in Reservoirs," *SPE Trans*, AIME (1973) 285,255.

[13] Adewole, E.S., Rai, B.M. and Audu, T.O.K.: " Mathematical Models of Selected Reservoir System involving Horizontal Wells," paper JSTR- 2002-81 accepted for publication in the *Journal of Science and Technology Research*.

[14] Adewole, E.S., Rai, B.M. and Audu, T.O.K.: "Well Test Analysis of Horizontal Well Subject to Simultaneous Gas Cap and Bottom Water Drive Mechanisms Using Type Curves," to appear in the *Nigerian Journal of Engineering Research and Development*, Vol.2, No. 4, 2003.

[15] Adewole, E.S., Rai, B.M. and Audu, T.O.K.: "Interference Test Analysis of Pressure Data from Lateral Wells in Layered Reservoirs with Crossflow," paper no. JSTR-2002-069 accepted for publication in the *Journal of Science and Technology Research*.

[16] Adewole, E.S., Rai, B.M. and Audu, T.O.K.: " The Use of Gauss-Legendre Quadrature in Solving Flow Problems in Horizontal Wells," *J. Nigerian Ass. of Mathematical Physics*, Vol.5 (Nov. 2001)89.